



# Sizes and relative geoeffectiveness of interplanetary coronal mass ejections and the preceding shock sheaths during intense storms in 1996–2005

J. Zhang,<sup>1</sup> W. Poomvises,<sup>1</sup> and I. G. Richardson<sup>2,3</sup>

Received 19 September 2007; revised 11 December 2007; accepted 27 December 2007; published 30 January 2008.

[1] We present a statistical study of the sizes of interplanetary coronal mass ejections (ICMEs) and the preceding shock sheath regions in near-Earth space. The 46 events studied are a subset of the events responsible for intense ( $Dst \leq -100$  nT) geomagnetic storms in 1996–2005 in which only a single ICME was responsible for generating the storm. We find that the durations and radial sizes of these ICMEs range from 8.0 to 62.0 hr and 0.08 to 0.63 AU, respectively, with average values of 30.6 hr and 0.37 AU. The sheath durations and radial sizes range from 2.6 to 24.5 hr and 0.03 to 0.31 AU, with average values of 10.6 hr and 0.13 AU. On average, the ICME radial size is 2.8 times that of the sheath. In terms of their relative geoeffectiveness, ICMEs contribute on average about 71% of the total energy input (sheath + ICME) into the magnetosphere. **Citation:** Zhang, J., W. Poomvises, and I. G. Richardson (2008), Sizes and relative geoeffectiveness of interplanetary coronal mass ejections and the preceding shock sheaths during intense storms in 1996–2005, *Geophys. Res. Lett.*, 35, L02109, doi:10.1029/2007GL032045.

## 1. Introduction

[2] Following initiation and acceleration close to the surface of the Sun, coronal mass ejections (CMEs) propagate through and expand in the heliosphere, where the ambient solar wind affects their subsequent kinematic and morphological evolution. These CMEs, also called ICMEs (interplanetary CMEs) in interplanetary space, often drive an upstream shock or wave and form a compressed sheath region between the shock/wave front and the driving ICME [Gosling *et al.*, 1990; Bothmer and Schwenn, 1996]. The magnetic and plasma properties of ICMEs and the associated sheaths, in particular the strength and duration of the dawn-dusk solar wind electric field, determined by the southward magnetic field component ( $B_s$ ), regulate the geoeffectiveness of these structures [Akasofu, 1981]. In this letter, we study the basic dimensional properties (duration and radial size) of both ICMEs and sheaths, and their relative geoeffectiveness. A statistical knowledge of these important parameters will help us understand the fundamental processes of CME evolution in interplanetary space.

[3] Because of the higher internal magnetic pressure with respect to the background solar wind, ICMEs expand with heliocentric distance [Bothmer and Schwenn, 1998; Liu *et al.*, 2005; Wang *et al.*, 2005; Forsyth *et al.*, 2006]. The pre-eruption CME structure, which lies close to the surface of the Sun, is usually only a fraction of a solar radius in size, e.g., the size of an active region or a filament. During eruption, a CME accelerates to hundreds of km/s and reaches a height of several solar radii in tens of minutes, driven by strong internal forces. The radial size of a CME is about a few solar radii at the end of the acceleration phase. This is followed by the so-called “propagation phase”, with relatively small changes of velocity and almost constant angular extension, whose small variations are largely influenced by the interaction with the ambient solar wind [Zhang and Dere, 2006]. Previous studies suggest that the average radial size of ICMEs at 1 AU is about 0.25 AU [Liu *et al.*, 2005; Forsyth *et al.*, 2006; Lepping *et al.*, 2006]. While a great deal has been learned about the size of ICMEs, the size distribution of the preceding sheath region is relatively less well studied. Nevertheless, it is known that the sheath size is equivalent to the standoff distance of a shock in front of an obstacle (in this case, the ICME itself) that depends on the shape of the obstacle and Mach number of the flow relative to the obstacle [Russell and Mulligan, 2002]. Furthermore, little is known about the relationship between these sizes and the properties of their solar drivers.

## 2. Observations

[4] The ICMEs used in this study are a subset of the 88 events that produced intense ( $Dst \leq -100$  nT) geomagnetic storms during 1996–2005 [Zhang *et al.*, 2007]. The interplanetary drivers of these intense geomagnetic storms fall into three broad categories: (1) “S-type” (53 events), in which the storm is associated with a single ICME and a single CME at the Sun; (2) “M-type” (24 events), in which the storm is associated with a complex solar wind flow which may include multiple ICMEs and sheaths, and may be the result of multiple halo CMEs launched from the Sun in a relatively short period which happen to interact with each other; and (3) “C-type” (11 events), in which the storm is associated with a corotating interaction region formed at the leading edge of a high speed stream originating from a coronal hole [Richardson *et al.*, 2006]. Note that a 5-category classification of solar wind drivers of geomagnetic storms, including moderate storms, has been made by Bothmer and Zhukov [2006, cf. Figure 3.53]. For the purpose of this study, we have used only the S-type events, because of the simplicity of the interplanetary driver, and because their size and driver structure are not affected by

<sup>1</sup>Department of Computational and Data Sciences, George Mason University, Fairfax, Virginia, USA.

<sup>2</sup>NASA Goddard Space Flight Center, Greenbelt, Maryland, USA.

<sup>3</sup>Center for Research and Exploration in Space Science and Technology and Department of Astronomy, University of Maryland, College Park, Maryland, USA.

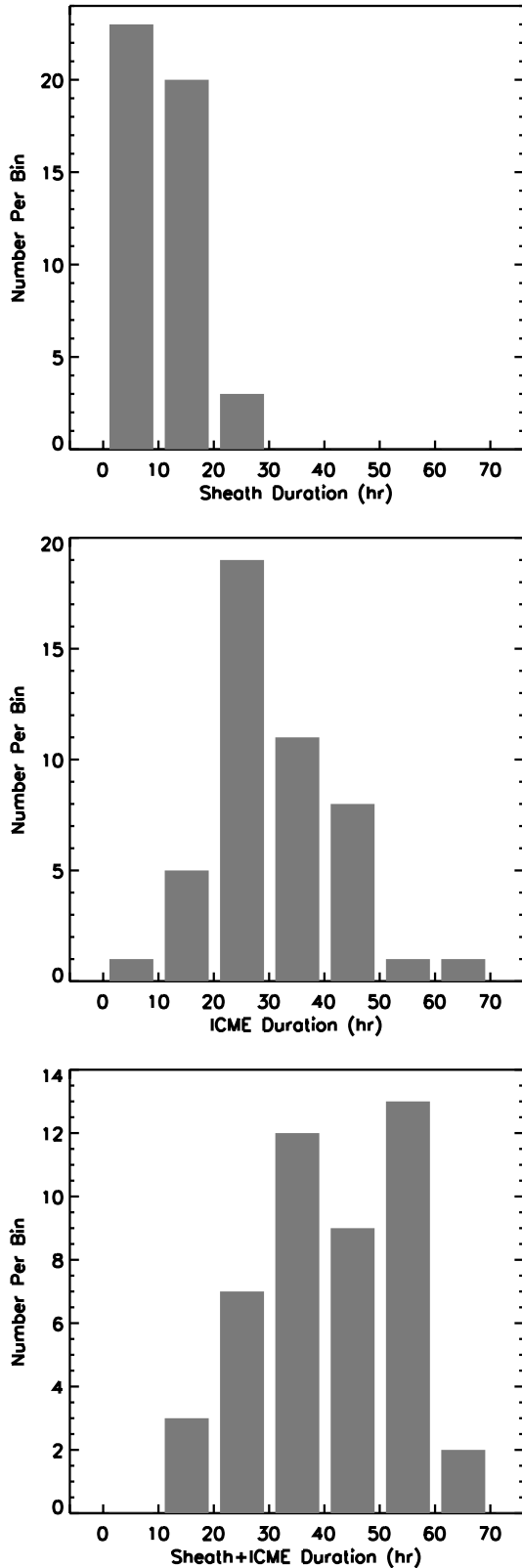


**Figure 1.** Distributions of the durations of (top) the shock sheaths preceding ICMEs, (middle) ICMEs, and (bottom) the entire transients (combined sheath and ICME) for the 46 single type solar-interplanetary drivers leading to intense geomagnetic storms in 1996–2005.

any preceding and/or trailing transients. Of the S-type storms, we here study the 46 events for which data are available from the ACE spacecraft.

[5] For each of these events, we identified three critical times: (1) The arrival time of the ICME-driven shock (or wave), giving the start time of the sheath; (2) The ICME arrival time, also indicating the trailing edge of the sheath, and (3) The ICME ending time. The shock/wave arrival time is obtained from examining the solar wind data upstream of the ICME for sharp discontinuities or more gradual increases in the solar wind speed, temperature, density and magnetic field intensity. We also referred to the ACE shock list ([http://www.ssg.sr.unh.edu/mag/ace/ACELists/obs\\_list.html](http://www.ssg.sr.unh.edu/mag/ace/ACELists/obs_list.html)). Note that preceding disturbances driven by slower ICMEs may not have steepened into shocks at 1 AU. To identify the start and end times of the ICME and hence estimate the duration of the ICME, we have used a combination of ICME signatures, including an enhancement of the magnetic field with a smooth rotation through a large angle, low field variance, abnormally low proton temperature and enhanced oxygen and iron charge states [Wimmer-Schweingruber *et al.*, 2006; Zurbuchen and Richardson, 2006]. We find that, although most of the signatures generally indicate a consistent starting time for a CME, the ending time may be less well defined. In this situation, for consistency, we use the trailing edge of the enhanced and smooth magnetic field to define the ending time of the ICME. Once the ICME region boundaries are identified, it is straightforward to calculate the linear size of the ICME features by integrating the observed solar wind speed with time during ICME passage (ACE data with 16-second resolution are used in this calculation). The size of the sheath can be determined in a similar manner.

### 3. Duration and Size of Sheaths and ICMEs

[6] The distributions in Figures 1 and 2 show, respectively, the durations and radial sizes of the sheaths, ICMEs and the sheath-ICME combined, for the 46 events studied. The total duration of the sheath and ICME has a wide variation from 12.9 to 66.2 hr with an average (median) value of 41.2 hr (41.6 hr). Most events (34/46, or 74%) have durations between 30 and 60 hours. The total sizes range from 0.12 to 0.73 AU with an average (median) value of 0.51 AU (0.51 AU). Most events (39/46, or 85%) have sizes between 0.3 and 0.7 AU. There are some events with remarkably long durations and/or large radial sizes. In particular, there are two events with durations of more than 60 hr, and four events with sizes larger than 0.7 AU.

[7] Considering the two components separately, the ICME durations range from 8.0 to 62.0 hr with an average (median) value of 30.6 hr (28.0 hr). The corresponding sizes range from 0.08 AU to 0.63 AU with an average (median) size of 0.37 AU (0.37 AU). The sheath durations range from 2.6 to 24.5 hr with an average (median) value of 10.6 hr (11.0 hr). Sheath sizes range from 0.03 AU to 0.31 AU, with an average (median) value of 0.13 AU (0.14 AU). The distributions of these sizes are not regular enough to allow a good functional fit to the profiles, mainly because of the limited number of events considered. Nevertheless, the average sizes calculated represent well the most probable sizes of these components as can be seen in Figures 1 and 2.

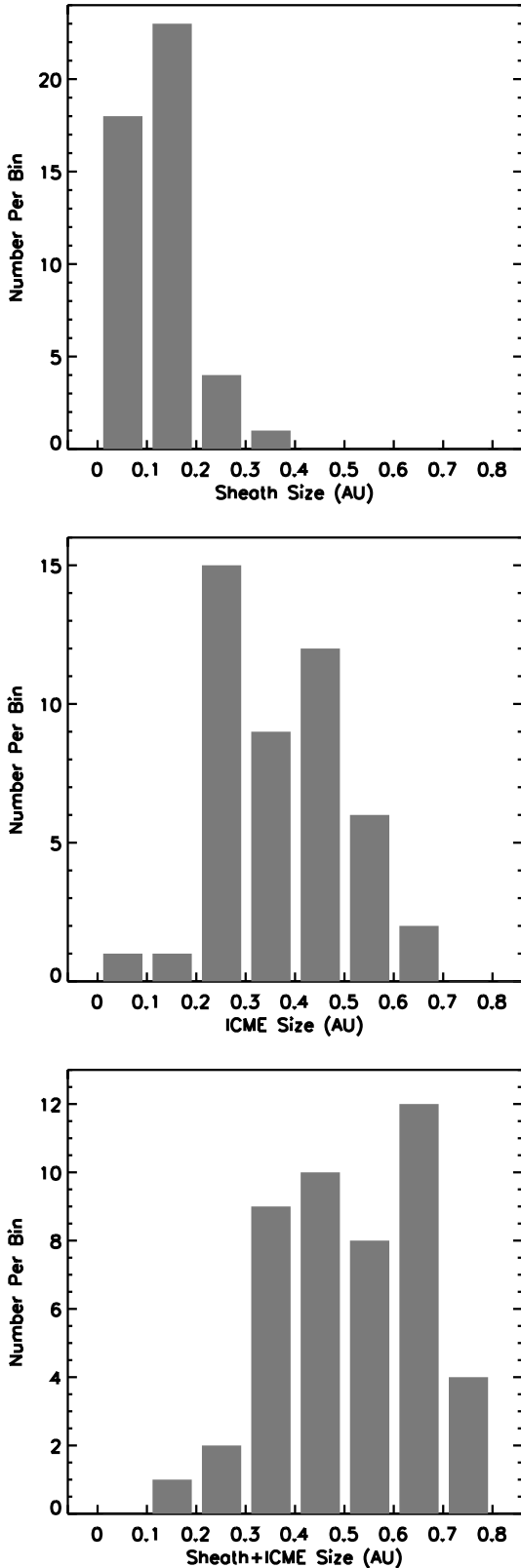


**Figure 2.** Distributions of (top) the radial sizes of sheaths, (middle) ICMEs, and (bottom) the entire transients.

The average size (duration) of the ICMEs is 2.8 (2.9) times as large as that of the sheaths. We do not find a correlation between ICME and sheath sizes or durations; the correlation coefficient is 0.06 for radial size and 0.21 for duration.

[8] We have also investigated the relations between the properties at 1 AU and that close to the Sun. However, the results obtained are generally of marginal significance. The ICME size has no correlation with the speed of corresponding source CME (correlation coefficient = 0.06). Furthermore, there is no correlation between the sheath size and the speed of the source CME at the Sun (correlation coefficient =  $-0.12$ ). Considering the geometric effects, we might have expected some relationship between ICME or sheath size and the longitude of source region, assuming this is a reasonable proxy for the direction of motion of the CME/ICME through the heliosphere. In particular, we might expect a spacecraft to pass through the nose of the sheath and central part of the ICME for an event originating near central meridian, and through the flanks of the shock and ICME for an event originating some distance from central meridian, potentially giving larger sheath and ICME durations and sizes. However, we find no correlation between ICME size and the longitude of the source CME (correlation coefficient = 0.09). A similar result is found between the sheath size at 1 AU and the longitude of the source CME (correlation coefficient = 0.11). There is a very weak negative correlation between the sheath radial size and the solar wind speed within the sheath (correlation coefficient =  $-0.26$ ).

#### 4. Relative Geoeffectiveness of Sheaths and ICMEs

[9] To estimate the geoeffectiveness of the sheaths and ICMEs, we use the well-known  $\epsilon$  parameter, which is a good proxy of the rate of energy input to the magnetosphere [Akasofu, 1981]. This parameter is given by

$$\epsilon = VB^2 \sin^4(\theta/2) l_0^2 \quad (1)$$

where  $V$ ,  $B$ ,  $\theta$ , and  $l_0$  denote the solar wind speed, the solar wind magnetic field magnitude, the polar angle of the magnetic field vector projected onto the Y-Z plane, and  $l_0 = 7 R_E$  (Earth radius). The solar wind parameters used here are in GSE coordinates rather than the usual GSM coordinates, in order to remove the seasonal effect due to the orientation of the Earth's dipole and thus focus on the intrinsic geoeffectiveness of the structure of interest. The total energy input during a certain period is obtained by integrating  $\epsilon$  during the period of interest. In Figure 3, we show the distribution of the total energy input provided by the sheath and ICME combined for 44 of the events studied (the plasma data are corrupted for the other events). The total energy inputs range from  $6.0 \times 10^{18}$  J to  $6.4 \times 10^{19}$  J with an average (median) value of  $1.4 \times 10^{19}$  J ( $1.3 \times 10^{19}$  J). Evidently,  $6.0 \times 10^{18}$  J is the lower cut-off of the energy distribution for these intense geomagnetic storms. There is a good correlation between the total energy and peak (minimum)  $Dst$  value (correlation coefficient =  $-0.68$ ). Such a correlation between the peak  $Dst$  value and the integrated input is expected since  $Dst$  is determined by similar parameters as  $\epsilon$ .

[10] In Figure 4, we show the distribution of the percentage of the total energy input into the magnetosphere contributed by ICMEs during these intense storms. The percentage due to ICMEs ranges from 2% to 99% with an average (median) value of 71% (80%). For about half of the events studied (23 out of 44), the ICME contributes more than 80% of the total energy input, whereas for only 2 events, the sheath contributes more than 80%. Evidently, the ICME usually dominates energy input into the magnetosphere during these storms. Nevertheless, sheaths remain an important energy source for these geomagnetic storms, contributing about 29% of the total energy input on average. It turns out that the relative contribution is mainly caused by the amount of the time spent within each of the structures. The power input, averaged with time, is almost equal in the sheath and ICME. It is about  $1.6 \times 10^{14}$  W in both components.

## 5. Summary and Discussion

[11] This study shows that there is a wide distribution in the radial sizes of both ICMEs (0.08 to 0.63 AU) and sheaths (0.03 to 0.31 AU), as well as the entire transients combining the two components (0.12 to 0.73 AU), associated with S-type intense geomagnetic storms. The average ICME size we obtain is 0.37 AU, which is significantly larger than, but not inconsistent with, the  $\sim 0.25$  AU size reported by other researchers [Forsyth *et al.*, 2006; Lepping *et al.*, 2006]. The difference may be a selection effect due to the fact that all the 46 events used in this study produced major geomagnetic storms, and thus may possess different properties, including perhaps a larger physical size that may help to sustain geoeffective solar wind conditions, than the general population of ICMEs. While ICMEs are the dominant transient features producing major geomagnetic storm, sheaths are also important, contributing about 29% of the total energy input into the magnetosphere during these storms.

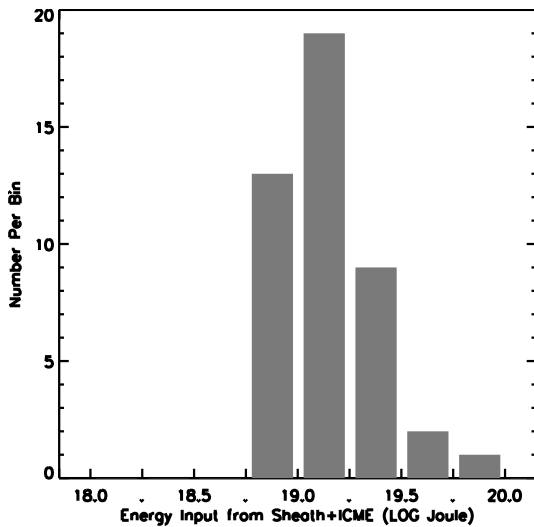


**Figure 3.** Distribution of the calculated total energy input into the Earth's magnetosphere from the entire interplanetary transients or sheath and ICME combined.

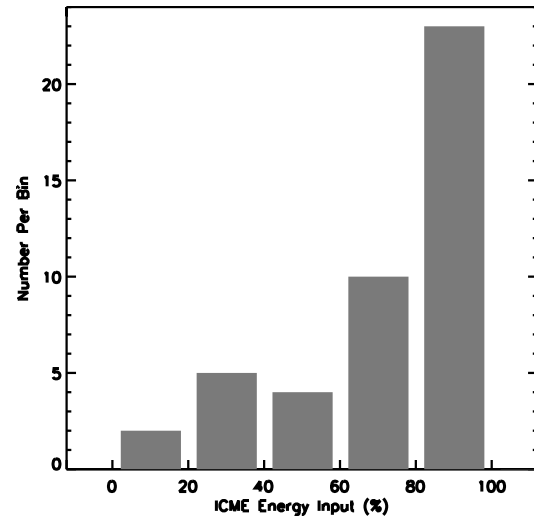


**Figure 4.** Distributions of the percentage of calculated energy input into the magnetosphere from ICMEs with respect to that from the sheath and ICME combined.

[12] The solar drivers of these transients are usually CMEs launched from the front-side of solar disk and with one part moving along the Sun-Earth line. However, we find that there is almost no correlation between ICME radial size and CME speed, even though CME speed is moderately correlated with the original CME size close to the Sun [Yashiro *et al.*, 2004]. Further, there is also no correlation between ICME size and the CME source longitude relative to central meridian, even though it might be expected that the spacecraft trajectory through the structures will influence the inferred size along this trajectory. Therefore, it seems that the size of ICMEs determined from observations at 1 AU is not well related to the CME speed and/or size observed by SOHO/LASCO coronagraphs close to the Sun. Several factors may be involved. The ICME size at 1 AU may be largely determined by its evolution in interplanetary space, for example, by the expansion rate, which depends on the pressure imbalance between the interior of the ICME and the ambient solar wind. The trajectories of the observing spacecraft may vary in latitude relative to the axis of the ICME, and this axis may also be inclined to the ecliptic.

[13] There is also almost no correlation between sheath and ICME sizes. This may not be too surprising since the dynamics controlling the evolution of ICMEs (e.g., expansion) [Forsyth *et al.*, 2006] and sheaths (e.g., compression, field line draping over the ICME) [Russell and Mulligan, 2002; Kaymaz and Siscoe, 2006] are totally different. We would expect the standoff distance between the shock front and ICME leading edge to increase as the angle between the nose of the shock and the observer increases, but this requires multiple-point observations of the same event.

[14] **Acknowledgments.** The ACE plasma and magnetic field data are provided by GSFC Space Physics Data Facility. SOHO is a project of international cooperation between ESA and NASA. J.Z. acknowledges the support from NASA grants NNG04GN36G and NNG05GG19G and NSF SHINE grant ATM-0454612. I.G.R. acknowledges a NASA Heliospheric Guest Investigator grant.

## References

- Akasofu, S.-I. (1981), Energy coupling between the solar wind and the magnetosphere, *Space Sci. Rev.*, *28*, 121.
- Bothmer, V., and R. Schwenn (1996), Signatures of fast CMEs in interplanetary space, *Adv. Space Res.*, *17*, 319.
- Bothmer, V., and R. Schwenn (1998), The structure and origin of magnetic clouds in the solar wind, *Ann. Geophys.*, *16*, 1.
- Bothmer, V., and A. Zhukov (2006), The Sun as the prime source of space weather, in *Space Weather: Physics and Effects*, edited by V. Bothmer and I. Daglis, p. 31, Springer, New York.
- Forsyth, R. J., et al. (2006), ICMs in the inner heliosphere: Origin, Evolution and propagation effects, *Space Sci. Rev.*, *123*, 383, doi:10.1007/s11214-006-9022-0.
- Gosling, J. T., S. J. Bame, D. J. McComas, and J. L. Phillips (1990), Coronal mass ejections and large geomagnetic storms, *Geophys. Res. Lett.*, *17*, 901.
- Kaymaz, Z., and G. Siscoe (2006), Field-line draping around ICMs, *Sol. Phys.*, *239*, 437, doi:10.1007/s11207-006-0308-x.
- Lepping, R. P., D. B. Berdichevsky, C.-C. Wu, A. Szabo, T. Narock, F. Mariani, A. J. Lazarus, and A. J. Quivers (2006), A summary of Wind magnetic clouds for years 1995–2003: Model-fitted parameters, associated errors and classifications, *Ann. Geophys.*, *24*, 215.
- Liu, Y., J. D. Richardson, and J. W. Belcher (2005), A statistical study of the properties of interplanetary coronal mass ejections from 0.3 to 5.4 AU, *Planet. Space Sci.*, *53*, 3, doi:10.1016/j.pss.2004.09.023.
- Richardson, I. G., et al. (2006), Major geomagnetic storms ( $Dst \leq -100$  nT) generated by corotating interaction regions, *J. Geophys. Res.*, *111*, A07S09, doi:10.1029/2005JA011476.
- Russell, C. T., and T. Mulligan (2002), The true dimensions of interplanetary coronal mass ejections, *Adv. Space Res.*, *29*, 301.
- Wang, C., D. Du, and J. D. Richardson (2005), Characteristics of the interplanetary coronal mass ejections in the heliosphere between 0.3 and 5.4 AU, *J. Geophys. Res.*, *110*, A10107, doi:10.1029/2005JA011198.
- Wimmer-Schweingruber, R. F., et al. (2006), Understanding interplanetary coronal mass ejection signatures, *Space Sci. Rev.*, *123*, 177, doi:10.1007/s11214-006-9017-x.
- Yashiro, S., N. Gopalswamy, G. Michalek, O. C. St. Cyr, S. P. Plunkett, N. B. Rich, and R. A. Howard (2004), A catalog of white light coronal mass ejections observed by the SOHO spacecraft, *J. Geophys. Res.*, *109*, A07105, doi:10.1029/2003JA010282.
- Zhang, J., and K. P. Dere (2006), A statistical study of main and residual accelerations of coronal mass ejections, *Astrophys. J.*, *649*, 1100, doi:10.1086/506903.
- Zhang, J., et al. (2007), Solar and interplanetary sources of major geomagnetic storms ( $Dst \leq -100$  nT) during 1996–2005, *J. Geophys. Res.*, *112*, A10102, doi:10.1029/2007JA012321.
- Zurbuchen, T. H., and I. G. Richardson (2006), In-situ solar wind and magnetic field signatures of interplanetary coronal mass ejections, *Space Sci. Rev.*, *123*, 31, doi:10.1007/s11214-006-9010-4.

---

W. Poomvises and J. Zhang, Department of Computational and Data Sciences, George Mason University, 4400 University Dr., MSN 6A2, Fairfax, VA 22030, USA. (wpoomvis@gmu.edu; jzhang7@gmu.edu)

I. G. Richardson, Code 661, NASA Goddard Space Flight Center Greenbelt, MD 20771, USA. (ian.richardson@gsfc.nasa.gov)